Available online at www.ijournalse.org

Emerging Science Journal

(ISSN: 2610-9182)

Vol. 10, No. 2, April, 2026

Thermoelectric Generator Efficiency Enhancement Through Copper Electrical Contact Optimization

N. Jagadesh Babu [1*], Rajesh Kumar Burra [1]

[1] *Department of EECE, GITAM (Deemed to be University), Visakhapatnam, Andhra Pradesh 530048, India.*

Abstract

Thermoelectric generators (TEGs) can transform heat into electricity and have considerable potential for diverse applications. Nonetheless, their widespread use is limited by their low efficiency, mainly owing to their high internal electrical resistance. This study aims to improve TEG performance by reducing the electrical contact resistance through the application of copper. This study addresses the critical challenge of improving the performance of thermoelectric generators (TEG) by reducing the electrical contact resistance, which directly affects the output power and conversion efficiency, particularly at low temperatures. The main objective of this study was to investigate how the contact resistance influences the electrical conductance and overall energy conversion efficiency of TEGs and to optimize the contact geometries to enhance the performance. Copper contacts with different shapes (flat and circular) were designed and fabricated to evaluate their impact on electrical resistance. Experimental investigations using a commercial TEG module were conducted to measure the contact resistances and analyze their effects on electrical parameters, including the output voltage, power, and conversion efficiency. A comprehensive theoretical model was developed to assess the contact area, energy loss, and thermal factors. Equations were applied to quantify the contact resistance and its influence on the power output and efficiency. Notably, small circular copper contacts exhibited a significant reduction in contact resistance compared to flat contacts, leading to an 18.6% improvement in efficiency at low temperatures. This study demonstrates that optimizing the geometry and size of copper contacts can substantially reduce energy losses at the interfaces, thereby enhancing the current flow and boosting the TEG conversion efficiency. These findings provide a novel approach for addressing the prevalent issue of high internal resistance in thermoelectric devices, paving the way for more effective energy harvesting and waste-heat recovery. This study underscores the critical role of contact engineering in TEG technology and offers promising strategies for improving device efficiency and output power for future applications.

Keywords:

Thermoelectric Generators;
Resistance at Contact;
Efficiency;
Electric Output;
Temperature Gradient;
Seebeck Effect;
TEG;
Figure of Merit.

Article History:

Received:	03	July	2025
Revised:	29	January	2026
Accepted:	14	February	2026
Published:	01	April	2026

1- Introduction

Thermoelectric generators (TEGs) enable the direct conversion of thermal gradients into electrical power through the Seebeck effect, offering significant potential for waste-heat recovery in automotive, industrial, and wearable applications. The intrinsic material figure-of-merit, ZT, fundamentally limits the ideal conversion efficiency of a thermoelectric leg; however, in practical modules, the realized efficiency is often significantly lower due to parasitic electrical and thermal losses at interfaces and contacts.

Recent studies indicate that electrical contact resistance (ECR) and thermal contact resistance (TCR) at the metal/thermoelectric and metal/heat-sink interfaces can substantially impact module-level performance losses, potentially negating improvements in material ZT if not adequately managed. Consequently, experimental and modeling efforts emphasize the necessity of incorporating contact resistances in performance assessments and module design [1].

* **CONTACT**: jnakka@gitam.edu

DOI: https://doi.org/10.28991/ESJ-2026-010-02-028

Extensive prior research has focused on reducing contact resistivity through interface engineering, such as the introduction of diffusion-barrier layers (e.g., Ni, Ni–P, multilayer Co–P/Ni–P), tailored metallization stacks, and surface treatments to achieve ohmic contacts and limit interdiffusion during thermal cycling. These studies report significant variations in specific contact resistivity depending on metallurgy, bonding method, and temperature, demonstrating that appropriate interlayers can achieve contact resistivities sufficiently low to approach device-limited performance in laboratory-scale demonstrations [2].

Moreover, the electrical physics of contact interfaces, notably current transfer length and current-crowding effects, result in non-uniform current injection that increases effective contact resistance unless electrode dimensions exceed characteristic transfer lengths. These phenomena suggest that geometry (pad area, pad thickness, fillets, vias, and the relative size of copper pads to TE legs) serves as a design lever with the potential to enhance module efficiency beyond what material improvements alone can deliver [3]. Comparatively few studies provide a systematic, quantitative linkage between copper electrode geometry (pad area, thickness, lateral extent, and filleting) and module-level ECR/TCR trade-offs under realistic operating conditions. Additionally, multi-physics coupling is underexplored in the context of geometry: while separate analyses exist for ECR, TCR, or geometric optimization, relatively few studies simultaneously model 3-D electrical spreading, Joule heating, and thermal constriction/spreading to quantify how geometric choices trade off electrical losses against thermal shunting. Furthermore, experimental validation and scaling remain inconsistent: measured contact resistivities and thermal contact conductance exhibit high variability across studies due to differing measurement methods, aging/cycling conditions, complicating the translation of small-coupon results to full-module geometry recommendations [4]. Model predictions will be validated against module-scale test cells to demonstrate the scalability of the geometry rules. By integrating precise contact metrology, multi-physics modeling, and experimental module validation, the proposed work aims to produce concrete, verifiable copper-contact design prescriptions that materially enhance practical TEG efficiency beyond materials-only improvements. The anticipated outcomes include validated correlations between copper pad geometry and effective contact-limited internal resistance and ΔT loss results, which will provide a crucial link between contact-material engineering and module-scale architecture, thereby facilitating more reliable and higher-efficiency thermoelectric modules for real-world applications [5]. Because they are capable of converting thermal waste energy to electrical power, there has been considerable interest in the field of thermoelectric generators (TEG) [6]. Theoretical thermoelectric generation is practical; however, low conversion efficiency limits its use [7, 8].

The junction between the thermoelectric elements and conductors where [9] electrical contact resistance occurs significantly affects the performance of the TEG systems. This investigation focused on increasing the efficiency of TEGs by improving the electrical contact geometry, with copper as the material of choice for these interfaces. A conscious change in the geometry and area of the contact interface may reduce the resistive losses and improve the overall efficacy of the system. Kramer et al. [10] integration of the theoretical analysis, experiments, and evaluation was applied. A new theoretical model was developed to quantify the impact of copper contact resistance [11] on TEG performance as the contact area changes, resistive losses, and thermal effects increase. The formulas for the electrical contact of the resistance, power output, and conversion efficiency calculation were developed for various contact geometries. The internal resistance is of key importance in the current flow in the TEG, thus influencing the overall output power.

This study used an experimental and simulation-based approach to validate the results of the proposed methodology. Using COMSOL Multiphysics, the electrical resistance of the contact and the resulting efficiency enhancements were simulated. Further experiments were conducted with prototype TEGs, each with a different contact area of copper, under conservative conditions. Further studies were conducted to compare the optimized contact geometry with commercial TEGs to determine its performance. This study applied statistical methods, such as error and regression analysis, to establish the validity of the model and test the electrical contact resistivity effects. This study aims to enhance high-performance thermoelectric generators for energy-harvesting applications.

2- Literature Review

Recent studies show that electrical contact resistance limits TEG efficiency. Copper is the best contact material because it conducts electricity and heat well, reducing losses. Simulations and experiments offer ways to improve this. Chen et al. [5] tested models for TEG circuits with copper wires. They found maximum power when load resistance equals the sum of internal, junction, and wire resistance. This means reducing copper contact resistance can improve power output and suggests revising circuit models to reflect real contact effects in TEGs [6]. The paper highlights that contact resistance at copper interfaces is a major barrier to efficient operation. Coelho et al. [6] used COMSOL simulations to study electrical contact resistance on copper-TE material junctions. They found power drops as contact resistance increases, with big losses over 50 $m\Omega \cdot mm^2$. Optimized copper contacts achieved Rc as low as 43–59 $m\Omega \cdot mm^2$, similar to modern devices, showing a strong link between simulated and experimental performance. A study introduced a simple block modeling technique for TEG modules with copper contacts. This method is accurate and allows quick studies of contact configurations. Adding metal foam heat exchangers with copper contacts increased

output power by 13% and efficiency by 9% in simulations. Physical experiments confirmed these models' accuracy, considering pressure-applied copper contacts and atmospheric effects [7]. Another paper used particle swarm optimization to improve TEG geometry and copper contact density. They found shorter legs with more copper contacts led to higher efficiency, showing contact density and distribution are key for optimization. The cross-sectional area and pressure at copper contacts affect electrical resistance and temperature uniformity, important for low-temperature operations [8]. Recent advances in flexible TEGs used hydrogel-copper foam composite sinks to improve heat dissipation and output power. Modeling showed copper foam's unique structure increases contact area, reducing electrical and thermal contact resistances and boosting efficiency, especially for wearable or low-power sensor applications [9]. Segmentation studies show electrical contact resistance at copper interfaces, usually in the range of $\Omega \cdot m^2$, is a major cause of efficiency loss at inter-material boundaries. Reducing both thermal and electrical resistances, through surface treatments or optimized pressure at copper contacts, improves peak power and efficiency in temperature gradients relevant to automotive and industrial systems [10].

TEG using a genetic algorithm. Increasing the contact resistance during research resulted in an 11.65% increase in the energy conversion efficiency percentage, underscoring its crucial function in performance evaluation [12]. The authors optimized a TEG system in which an instantaneous efficiency of approximately 6.5% was realized, which improved the thermal-to-electrical energy conversion [13]. In this work, the authors studied high-copper alloys used in automotive connectors to maximize the mechanical and electrical properties there by increasing the value of improving the efficiency of thermoelectric generators. This study measured changes in the electrical contact resistance, using only theoretical evaluations [14]. The optimization of the contact resistance in this study was uncoupled. The maximum generated power output of 70.81 mW was recorded at a hot end temperature of 200°C, which is high for the basic unicouple of TEG [15]. In this study, the authors reported that high electrical and thermal contact resistances negatively impact the thermoelectric device performance, making the optimization of joining methods essential. An Ag water-based material was used. Computer simulations indicated that high contact resistance significantly reduce the power output of thermoelectric devices., with an efficiency of 12.4% [16]. In this research, the author reported that the overall efficiency of the proposed exhaust thermoelectric generator (ETEG) system is 7.81%, which is a crucial factor in its operation and performance. The efficiency difference between the maximum efficiency and total efficiency increases from 1.5% at a low temperature difference of 100 K to 12.67% at a high temperature difference of 800 K, and this is the very high temperature considered [17]. The authors investigated the resistances to heat and reported that reducing the electrical and thermal resistances at the contacts and interconnectors to reasonable values can greatly increase the efficiency of small thermoelectric modules. The impact of undesired resistances is considered in an enhanced method for calculating the maximum efficiency of 11.8%. [18].

In this work, the author reported that the optimization of electrical contacts in thermoelectric generators is crucial for maximizing the output power and efficiency and for optimizing the load resistance. Circuits were designed as an equivalent electric circuit model that can effectively support the design and optimization of thermoelectric systems by addressing both thermal and electrical issues. A dc-dc circuit was used. Through the PSpice [19] to increase efficiency, the author of this work presented a miniature thermoelectric generator (TEG) that transforms thermal energy into electrical energy. The TEG submodel enables biological analysis of the implants and enhances the overall performance of the generator [20]. In this study, the electric current significantly influences the friction coefficient in the electric contacts of a TEG, and the electrical current has a significant impact on the electrical resistance of the contact in the TEG and does not have statistical parameters [21]. To improve performance measures such as the dimensionless output power and thermal efficiency, the maximum efficient power of a two-stage TEG decreases from 0.308 to 0.2381 W [22]. The fabrication process of the copper–graphite composite was optimized in this study significantly; the electrical conductivity and wear resistance of the composite were significantly improved by varying the graphite percentage, sintering temperature, and compaction pressure. The compaction pressure was 750 MPa, the sintering temperature was 950°C, and a high temperature was used in this case [23]. In this study, the authors theoretically reported that decreasing the electric contact resistance leads to increased efficiency and effectiveness of thermoelectric generators (TEGs). A suitable ratio of the cross-sectional area enhanced the output power and efficiency of the TEG device through cascaded ANSYS simulations [24]. This study investigated the performance of Peltier elements in improving the energy generation efficiency of thermoelectric generators. A mathematical model was developed to analyze the energy conversion accuracy and influence of temperature gradients on efficiency [25, 26].

3- Research Methodology

The methodology for improving the thermoelectric generator (TEG) efficiency through the optimization of the electrical contact geometry involves several steps. After researching the effects of thermoelectric effects and micro energy generation through energy harvesting, an analytical model of a TEG was constructed via the classical theory of steady-state analysis of electrical circuits [10]. The text describes the creation of a theoretical model for a TEG. This model was developed via well-established principles from electrical circuit analysis, specifically focusing on steady-state conditions. In this study, two concepts are referred to as thermoelectric effects. These are phenomena where

temperature differences in materials can create electrical voltage, or vice versa. Figure 1 shows the flowchart of the research methodology through which the objectives of this study were achieved.

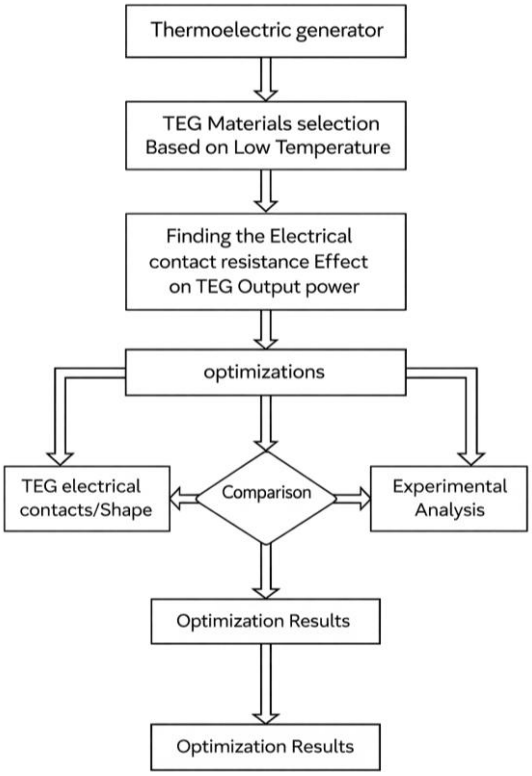

Figure 1. Methodology of thermoelectric generators contact electrical resistance optimization

The study follows a structured approach to enhance thermoelectric generator (TEG) efficiency at low temperatures by focusing on electrical contact resistance, The principle and operation of TEGs are established, emphasizing their conversion of thermal gradients into electrical energy.

Material Selection: Thermoelectric materials that can function at low temperatures, often based on bismuth telluride, are selected by taking conductivity and the Seebeck coefficient into account.

The main reason copper is chosen for electrical contacts in low-temperature thermoelectric generators (TEGs) is its high electrical conductivity, which reduces Joule heating losses—an important factor given the inherently low voltage output of TEGs. Additionally, copper has excellent thermal conductivity, ensuring uniform temperature distribution and efficient heat transfer at contact interfaces. Furthermore, its favorable mechanical properties, compatibility with fabrication processes, and reasonable cost make copper suitable for both commercial and manufacturing applications, effectively balancing performance and cost.

Compared with other materials such as silver, nickel, and aluminum, copper offers a more practical combination of properties. Nickel, although it has superior oxidation resistance, has lower electrical conductivity and higher resistive losses, and is therefore often used as a barrier layer. Aluminum has good thermal properties but suffers from rapid oxide layer formation, which increases contact resistance—especially at low temperatures. Silver provides the highest electrical and thermal conductivities; however, it is cost-prohibitive and susceptible to electromigration, limiting its widespread application.

Oxidation remains a key concern, as it leads to the formation of surface oxides that increase electrical contact resistance over time, particularly under thermal cycling or humid conditions. To assess the impact of contact resistance, analytical models and simulations are used to quantify its effect on TEG output power and efficiency. Optimization processes are computational, employing multi-parameter optimization techniques to propose improved contact designs and minimize resistance. Geometry and shape analyses are conducted to tailor contact configurations and interface features, guided by simulation results. Experimental validation involves fabricating prototypes and testing their electrical and thermal performance. Theoretical predictions are then compared with experimental data to validate models and refine designs. The final stage involves reporting the results, presenting the optimal configurations supported by quantified improvements in power output and conversion efficiency.

This methodology integrates simulation, design, and experimental validation in a cyclic workflow, leading to well-supported recommendations for reducing electrical contact resistance and enhancing TEG efficiency.

3-1- Theoretical Modeling

A mathematical model was formulated to assess the influence of the copper contact resistance on the thermoelectric generator efficiency. The electrical contact resistance, power output, and conversion efficiency equations were formulated based on the different contact geometries. The criteria for review include differences in contact areas, such as electrical contact resistance, as shown in Figure 2. Electricity the oxidation occurs at the interface between the thermoelectric material and metallic electrodes. This causes Joule heating and voltage drops there by reducing the useful [17] power output. COMSOL Multiphysics software was used to simulate the electrical contact resistance and improve efficiency. Virtual models of the TEG modules with varying copper contact areas and geometry were created. The impact of different contact designs on the overall system performance was analyzed. For experimental validation, commercial TEG modules with different copper contact areas and geometry designs were used, and a controlled testing environment was set up to measure the TEG performance [18]. Experiments were conducted to measure the electrical resistance, power output, and conversion efficiency. Data from multiple trials were recorded and analyzed to ensure reproducibility.

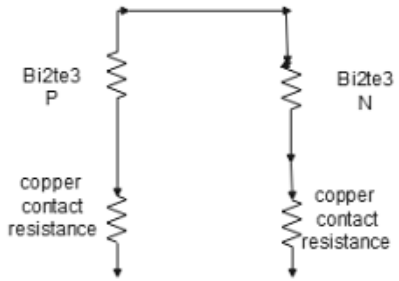

Figure 2. Thermoelectric generator resistance analytical model

Mathematical Modeling and Analysis:

The electrical contact resistance R_C can be calculated as follows ρ_c:

$$R_C = \frac{\rho c}{A} \quad (1)$$

where, R_C = Contact resistance (Ω); ρ_C= Contact resistivity (Ω.m); A = Contact area ($m m^2$).

Based on the results shown in Figure 2, the contact resistance is expressed in Equation 1, and the contact resistance R_C - depends on the contact resistivity and contact area of the thermoelectric generator P,N legs.

Thermoelectric Efficiency:

$$\eta = \frac{P_{Out}}{Q_{in}} \quad (2)$$

where; η = Efficiency; P_{Out} = Electrical power output (w); Q_{in} = Heat input (w); P_{Out} = is the output power.

$$P_{Out} = \frac{2(S\Delta T)^2}{R_t} \quad (3)$$

Equation 1 is the thermoelectric generator conversion efficiency, which converts heat energy in to electrical energy (generated power). where; S=Seebeck coefficient ($\frac{V}{K}$); ΔT = Temperature difference (k); R_t = Total resistance($R_C + R_{TE}$); Thermal drop at the interface (ΔT) ΔT_{drop} = Q.R_{tc}; Effective temperature gradient Δ_{Teff} =$\Delta T - Q.R_{tc}$; Voltage drop from the electrical contact resistance V_{drop} = I.R_c.

Here, Equations 2 and 3 represent the thermoelectric generator efficiency and power output through the Seebeck effect 's'. The temperature gradient 'ΔT' is the difference between the hot and cold temperature.

$$\text{Power output: } P = \frac{(V_{oc})^2 R_{Load}}{(R_{Load+} + R_c + R_{int})^2} \quad (4)$$

Equation 4 expresses the electrical power of the thermoelectric generator, which is the electrical power equation related to the voltage, current and Ohm's law combination of parameter resistances, with the Seebeck effect behind the principle.

$$\text{Efficiency: } \eta = \frac{\Delta T}{T_H} \frac{\sqrt{1+ZT}-1}{\sqrt{1+ZT+\frac{T_C}{T_H}}} \quad (5)$$

The temperature coefficient of resistivity for copper is 0.00393/k. Equations 4 and 5 indicate that the power generation efficiency of the thermoelectric generator behind this principle is the Seebeck effect. One of these parameters affects the materials.

Case 1: Copper contact geometry effects on the figure of merit ZT

Temperature affects the copper electrical contacts in TEGs and has implications for the figure of merit (ZT) of thermoelectric generators.

Figure of merit $ZT = \frac{S^2 \sigma T}{K}$ (6)

Equation 6 shows that the ZT values vary owing to the TEG electrical conductivity of the copper material with the geometry of the copper contacts of the thermoelectric generator [27]. Here, we need to increase the electrical contacts of the copper contacts at different temperatures, subsequently as the temperature increases, the electrical resistance of the copper increases. In the TEG, the contacts of the copper resistivity 'ρ_c' depend on the TEG temperature T_H, T_C .

3-2-Simulation Validation

COMSOL Multiphysics packages for electric circuits and the thermoelectric effect in steady-state scenarios were used to create a geometric model. The thermoelectric effect was assumed to be solely caused by bismuth telluride in the materials of the legs maintaining the same size and thermoelectric properties [28] similar to the analytical model. It was assumed that all the ceramic plates were at the same temperature [29]. Unlike the analytical model, this model contains thermal and electrical contact resistances as well as temperature-dependent changes in material properties (such as electrical conductivity and the Seebeck coefficient) that are obtained from the inherent data of the program used. COMSOL Multiphysics was used to simulate electrical contact resistance and related efficiency gains.

Here, as in Figure 3, the thermoelectric generator's analytical model was created to produce electricity from the waste heat energy of low temperatures, with a primary focus on the generated electrical output pickup through copper electrical connections that have resistances. These resistances affect the generated electrical conversion efficiency of the TEG, as shown in Figure 3. The geometry dimensions of the thermoelectric generator electrical contacts were designed, and changes were studied through this design. The simulation in COMSOL Multiphysics can provide valuable insights into the relationship between electrical contact resistance and efficiency improvements in thermoelectric generators. By analyzing the temperature distribution and electrical characteristics [26] of the system, researchers can optimize the design [27] of copper electrical contacts to minimize resistance losses. This analytical model can be particularly useful for studying the impact of varying contact geometry dimensions on the overall performance of thermoelectric generators operating in low-temperature waste heat recovery applications.

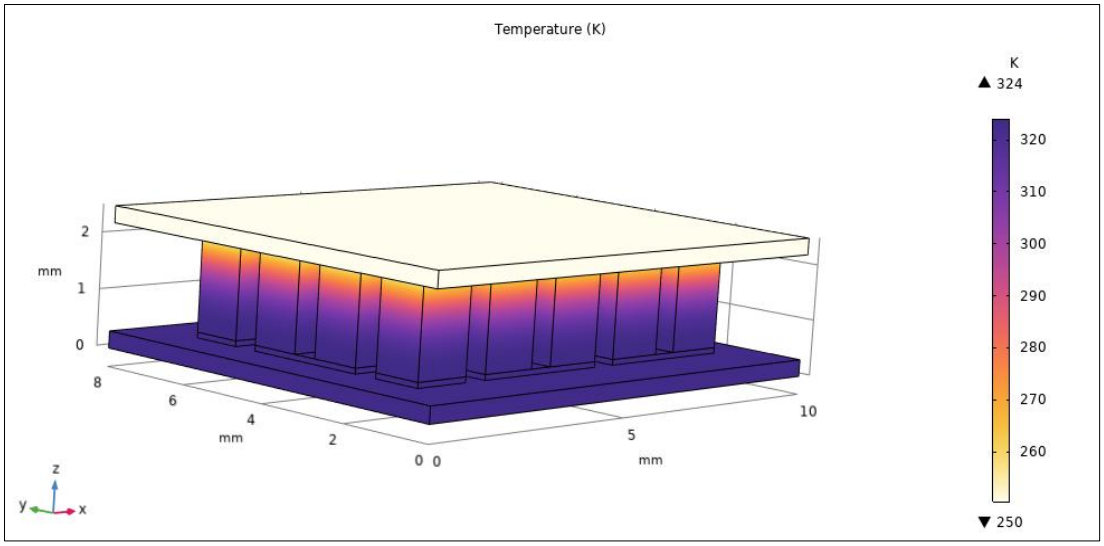

Figure 3. Thermoelectric generator temperature (K) analytical model

3-3- Geometry and Material Selection

The TEG model consisted of one p-type and one n-type thermoelectric leg sandwiched [27] between two ceramic plates with metal contacts. The materials used were as follows: n-type leg bismuth telluride ($Bi_{2\,Te_3}$based), p-type leg, contact metals (copper), and ceramic plates (alumina) [30, 31].

Governing Equations for COMSOL Multiphysics

COMSOL solves the coupled electrothermal equations. The relevant physics interfaces used include Heat Transfer in Solids: $\rho C_p U \nabla T + \nabla . q = Q + Q_{ted} : q = -\nabla T$, Electric currents: $\nabla \cdot J = QJ.V, J = \sigma E + Je.$

$$E = -\nabla V \tag{7}$$

Thermoelectric effects: considered for the design to generate electric power from the temperature gradient in COMSOL Multiphysics: $P = S\,T$ and $q = P\,J$

$$e = -\sigma S \nabla T \tag{8}$$

The contact resistances are modeled as thin resistive layers at the interfaces. The thermal contact resistance is modeled via a layer boundary condition with a specified thermal contact. As Figure 4 the temperature conduction from hot temperature to cold temperature to electrical contact resistance is included via boundary conditions with surface resistivity. Boundary conditions, Response. The bottom ceramic plate tracks a constant cold-side and hot-side temperature [26] the electrical load is connected between the metal contacts. Mesh, refined at contact interfaces for better accuracy. Study Type, Stationary analysis.

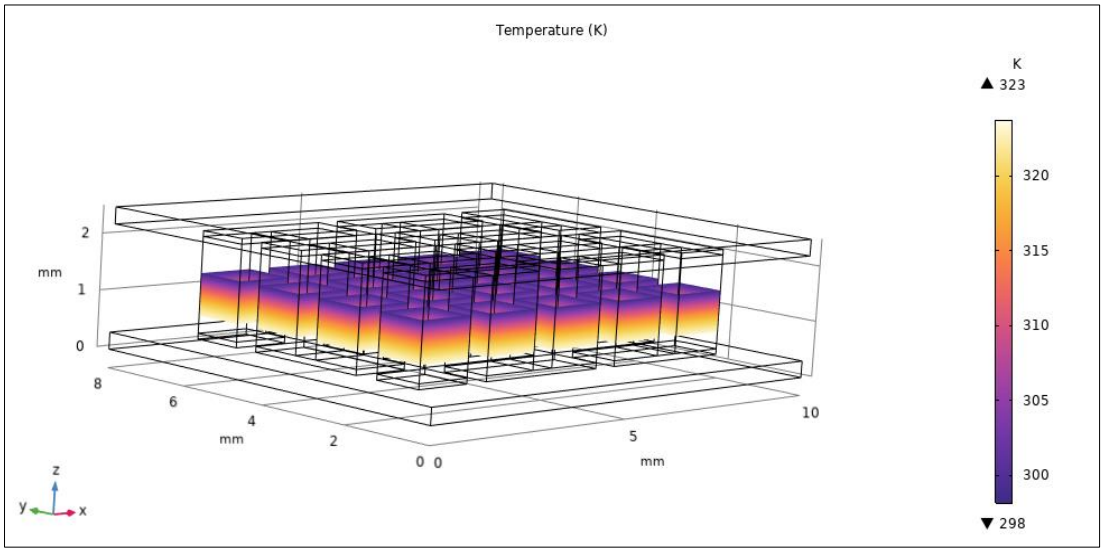

Figure 4. Thermoelectric generator: Heat transfer (K) analytical model

Error analysis was performed to quantify the uncertainties in the measurements and calculations. As Figure 5 conducting a regression analysis to establish relationships between the contact geometry parameters and TEG efficiency. The model's accuracy and reliability were validated via statistical methods.

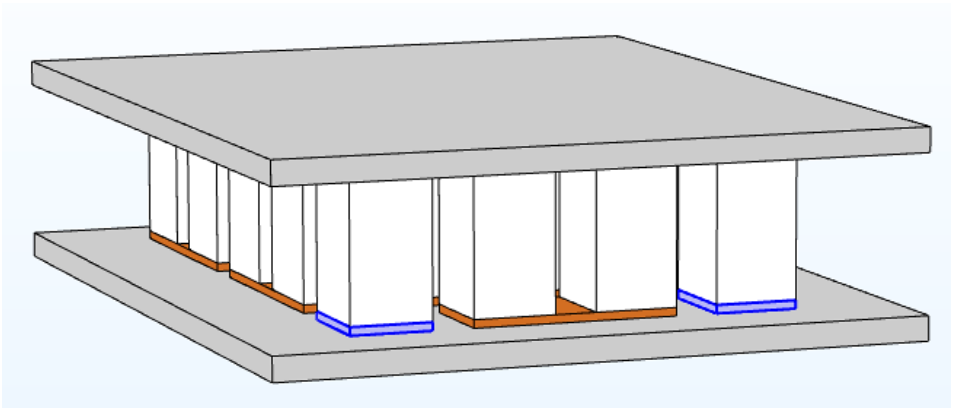

Figure 5. Thermoelectric generator, flat-type contacts, analytical model Geometry (mm)

3-4- TEG Model Validation

Different types of validations were used to test the TEG contact resistances of the thermoelectric flat type(shape) copper contact designs, different sizes of copper contact dimensions were used, and the corresponding changes in electrical contact resistances were [32] determined. The results of the electrical contact resistance test are shown in Figure 6. The TEG was designed by meshing the TEG in COMSOL solids and contact-resistance boundary conditions under the heat transfer of a TEG [33].

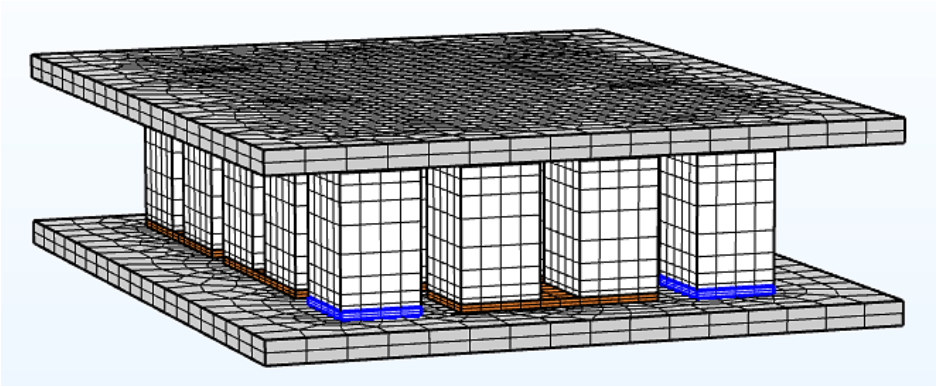

Figure 6. Thermoelectric generator, flat-type contacts (mm), analytical model with fine mesh

In case-1, a thermoelectric generator with flat-type electrical contacts was designed and analyzed, with geometrical variations in the contacts. In this Table 1 the contact resistance varied with the thickness of the flat type regular contact of the thermoelectric generator. Electrical contact resistance: Electrical contact resistance leads to a voltage drop and ohmic losses, reducing the output voltage and efficiency. Power delivered to the load:

$$\frac{(V_{oc})^2 R_{load}}{(R_{load}+R_C+R_{int})^2} \quad (9)$$

Here R_{int} is neglected; R_C = electrical contact resistance (Ω)I = current; V_{oc}= Open circuit voltage; R_{Load} = external load resistance; V_{drop}=I.R_C. The effective voltage across the load reduces the output power. Contact Geometry Optimization: The optimized contact area A_{Opt} can be modeled as R_C. From Figure 5 the thermoelectric generator generates the output power an open circuit, as shown in Table 1. Variable resistance values were used to calculate the TEG output power. Here we can consider Equation 10 as the contact resistance and then calculate the thermoelectric power. where R_C is the resistance of copper. The results of the contact resistances measured for different contact designs were as follows: flat and circular type with various geometries.

$$R_{Contact} \quad R_C \frac{\rho_c}{A} \quad (10)$$

In case-1, the contact resistance increases, with increasing contact area according to Equation 11:

$$A_{Opt}=\frac{\rho_c}{R_C} \quad (11)$$

where; ρ_c Contact resistivity of copper.

Table 1. Thermoelectric generator electrical flat type contact geometry (mm) vs. resistance R_c(Ω)

S. No.	Flat Type Contact Thickness (mm)	Resistance (Ω)
1	0.1	0.081
2	0.2	0.086
3	0.3	0.098
4	0.4	0.12
5	0.5	0.18
6	0.6	0.22
7	0.7	0.31
8	0.8	0.40
9	0.9	0.42
10	1.0	0.47
11	1.1	0.49
12	1.2	0.51
13	1.3	0.52
14	1.4	0.56
15	1.5	0.63

After designing TEGs with flat-type electrical contacts of different thicknesses, the contact resistance at the interface of the TEG was studied, and the corresponding TEG efficiency was also studied. From Figure 7 the analysis of the regular flat-type contacts of the TEG reveals that the contact resistance increases with increasing thickness of the regular

flat-type contacts of the TEG. This increased contact resistance affects the output power generation of the TEG. Here we observed that increasing the contact resistance reduces the output power and conversion efficiency.

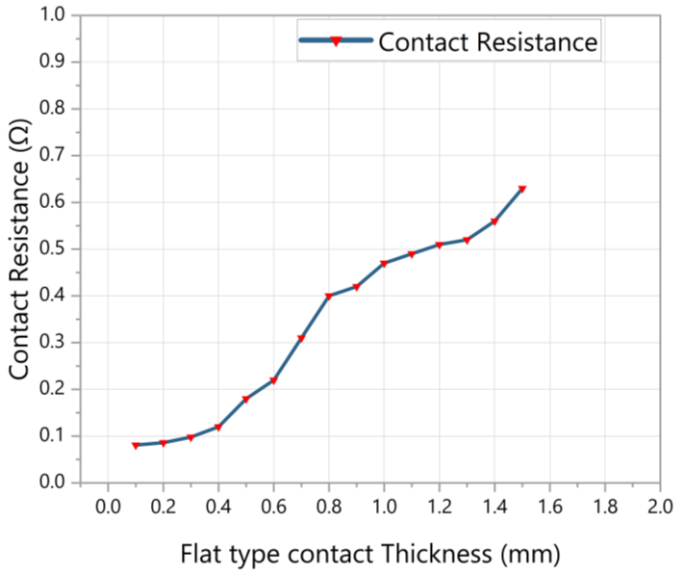

Figure 7. TEG flat-type copper contact geometry (mm) vs. Contact resistance (Ω) analytical model

Case 2: Optimization of the circular contact geometry TEG design module

In case -1, we designed a thermoelectric generator with a regular flat-type contact geometry and analyzed the contact resistance, which affects the TEG output power and conversion efficiency at low temperatures (constant temperatures). After this observation we need to optimize the TEG through contact geometry and shape. The TEG parameters of the TEG power output and conversion efficiency can significantly be enhanced by optimizing the electrical contact geometry [34]. Researchers can minimize parasitic losses and improve the overall performance of the system by lowering the contact resistance.

Considering Equation 2, a thermoelectric generator with a circular shape and geometry was designed: $R_C = \frac{\rho_c}{A}$: 'A'- is the cross-sectional area A, Copper is used for electrical contact; its resistivity increases with temperature: $\rho_{(T)} = \rho_{0\,[1+\propto(T-T_0)]}$, where $\rho_{(T)}$ is the resistivity at temperature T and where ρ_0 is the resistivity at the reference temperature T_0.

From Figure 8, the design of a thermoelectric generator with circular-shaped contacts and geometry for optimizing TEG output power and conversion efficiency is shown. A temperature measuring device based on the principles of heat conduction and convection surface temperature averaging was used for measurement in the case of a TEG. This was the primary objective of this simulation.

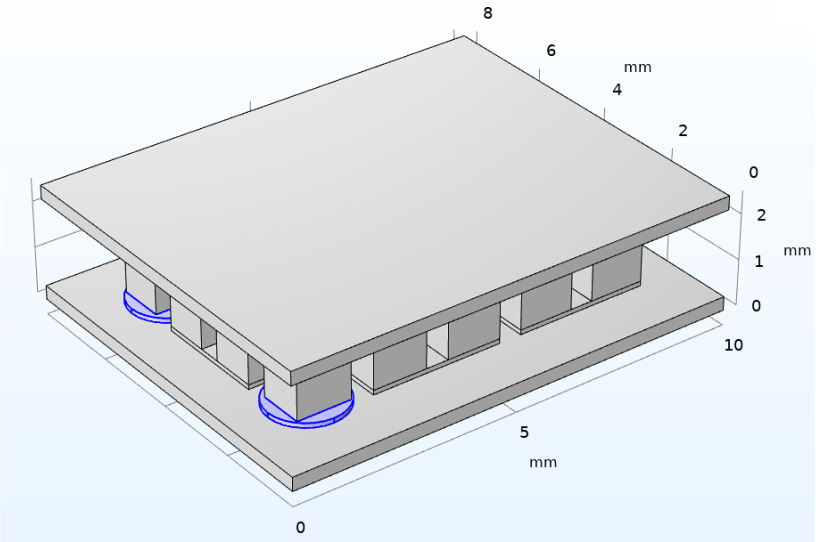

Figure 8. Analytical model of the thermoelectric generator circular-type contacts (mm)

Here is the thermoelectric generator with circular contacts with variable hot temperatures. The system works in a quasistationary regime for different mechanical contact configurations of the thermoelectric modules. The thermal interface was defined as the ambient temperature (room temperature) and heat source with controlled fixed temperatures of 298 K and 323 K for the heated surface and the cold source, respectively. It was believed that the module would have a cohesive mesh for defining the thermoelectric properties. Only the resistance resulting from contact with copper is included; internal electrical and thermal resistances are assumed to be zero (see Figure 9).

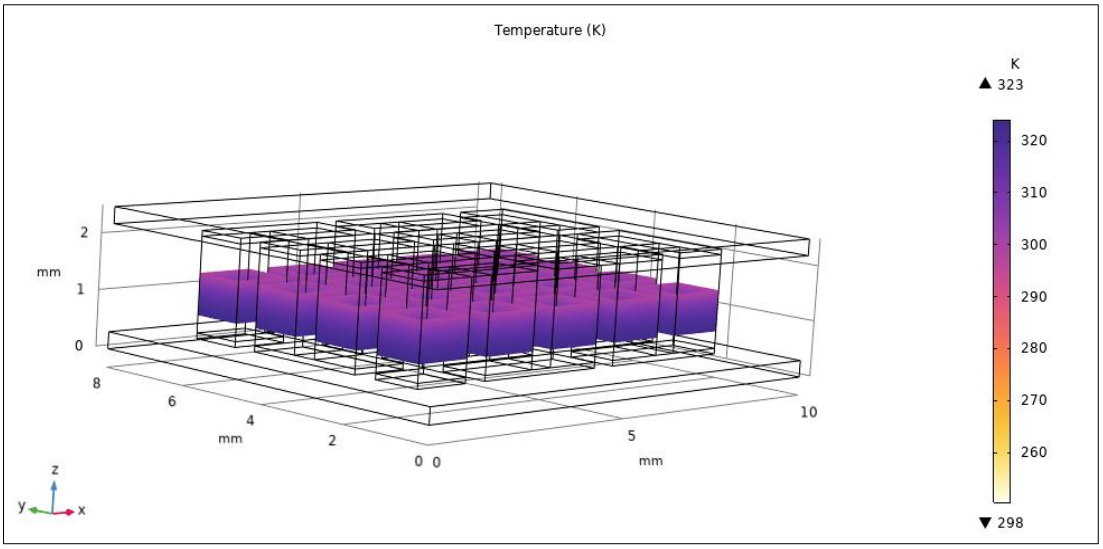

Figure 9. Thermoelectric generator, Circular type contacts (mm), Analytical temperature(K)model

Because thermoelectric devices are thermally connected in parallel and electrically coupled in series, the voltage potential fluctuates from one end of the model to the other. Although much work has been done to study the efficiency of thermoelectric systems, the geometric configurations of changing the cross-sectional areas of thermoelectric contacts have not received significant attention in the reviewed literature. Therefore, the purpose of this research is to thoroughly investigate the effects and operation of thermoelectric generators utilizing new electric contact geometries that have not yet been discussed in the literature. Both the traditional rectangular shape as a reference module and novel configurations, such as the circular shape using COMSOL Multiphysics, He & Tritt [35] were among the TEG electrical contact geometries investigated. Examination of voltage potential and temperature distributions.

Figure 10, plotting the current output against the temperature differential between the hot and cold sides of the device in the graph above demonstrates how a TEG is characterized. The graph displays the typical behavior of current generation as ΔT increases.

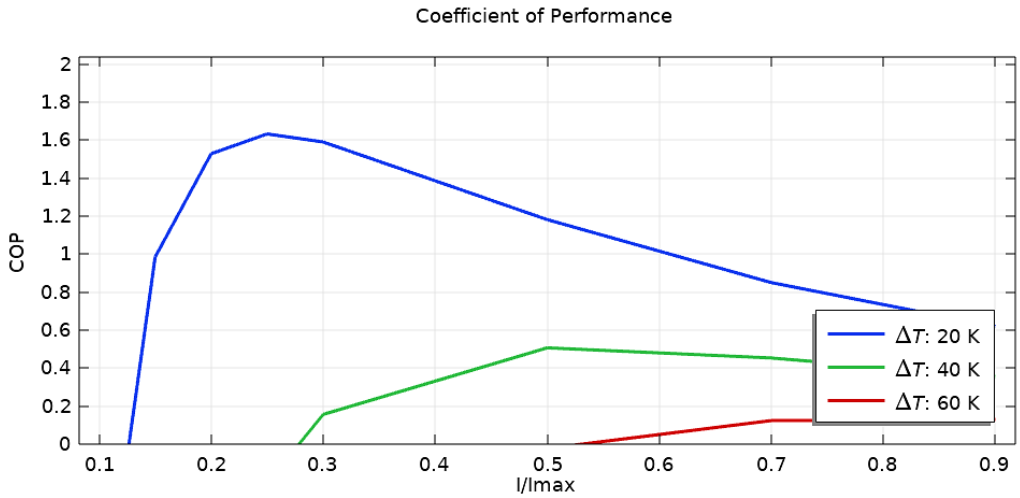

Figure 10. Thermoelectric generator COP Vs Generated Current at Different ΔT (K)values

Figure 11 shows the current generated from different ΔT values. At low ΔT, the current increases nearly linearly with increasing Seebeck effect voltage. At a higher ΔT, the current growth may begin to saturate owing to increasing internal resistance, material limitations, and heat losses.

Thermoelectric generator:

$$\text{Efficiency } \eta = \frac{\Delta T}{T_H} \frac{\sqrt{1+ZT}-1}{\sqrt{1+ZT+\frac{T_C}{T_H}}} \quad (12)$$

$$\text{Figure of merit } ZT = \frac{S^2 \sigma T}{K} \quad (13)$$

On the basis of simulation, experimentation, and analysis results, the optimal contact geometry for maximizing TEG efficiency can be identified. The resistance R contact, $R = \rho \frac{l}{A}$: 'R' is the resistance Ω, and 'ρ' is the electrical resistivity of the TEG contact copper. 'L': length of the TEG electrical contacts; 'A' is the cross-sectional area of the electrical contact of the thermoelectric generator with copper.

To optimize TEG electrical contacts, a conductance improvement for the thermoelectric generator and efficiency improvement are needed. The geometry was changed to obtain the required power output of the TEG based on the temperature gradient input. Cross-sectional area of TEG electrical contact of copper A.

$$\text{Area } A = \pi r^2 \quad (14)$$

where, r is the radius of the electrical contacts of the TEG.

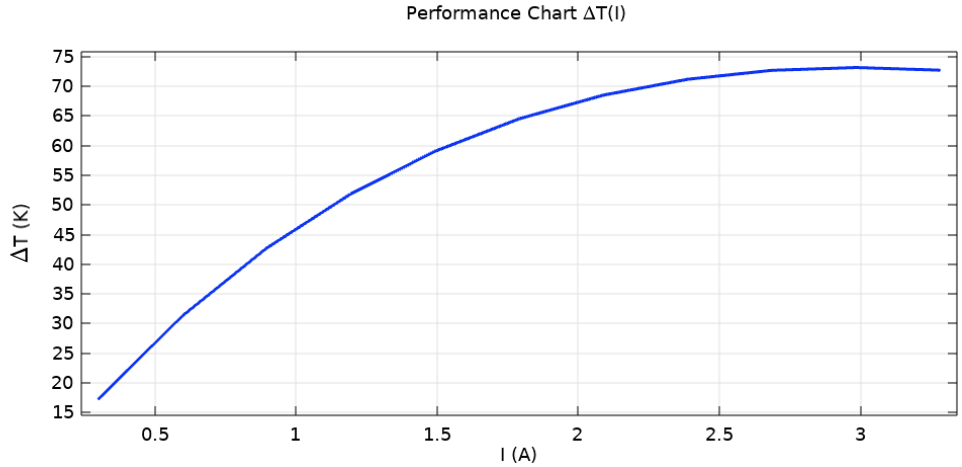

Figure 11. TEG Temperature gradients ΔT(K) Vs Generated Current I(A)analytical model

Table 2, the contacts had a circular shape, and the resistance varied with the circular area of contact of the thermoelectric generator. The improvement in the efficiency of a TEG depends on one of the key parameters, The electrical contacts of the copper. With respect to the electrical contacts of the copper optimization for improving the thermoelectric generator efficiency, a different geometry of the contact area is designed to change the output resistance to improve the output power and thermoelectric generator efficiency.

Table 2. Thermoelectric generator electrical circular type contact geometry (mm) vs. resistance R_c(Ω)

O	Radius r (mm)	Area (mm^2)	Resistance (Ω)
1	0.1	7.85×10^{-9}	0.68
2	0.2	3.14×10^{-8}	0.53
3	0.3	7.06×10^{-8}	0.23
4	0.4	1.25×10^{-7}	0.13
5	0.5	1.925×10^{-7}	0.09
6	0.6	2.826×10^{-7}	0.05
7	0.7	3.846×10^{-7}	0.04
8	0.8	5.02×10^{-7}	0.03
9	0.9	6.35×10^{-7}	0.026
10	1.0	7.85×10^{-7}	0.011
11	1.1	9.49×10^{-7}	0.014
12	1.2	1.13×10^{-6}	0.014
13	1.3	1.32×10^{-6}	0.012
14	1.4	1.53×10^{-6}	0.01
15	**1.5**	$\mathbf{1.76\times10^{-6}}$	$\mathbf{9.51\times10^{-3}}$

Figure 12 shows the change in resistance of the electrical contacts from the optimized geometry area of the electrical contacts of the TEG. Here, the change in resistance [36] has an impact on electrical conductivity, which affects the thermoelectric generator power conversion from the input of the waste heat source, and then this electrical contact resistance changes the thermoelectric generator efficiency: Conductivity σ, $\sigma_C = \frac{1}{R_C}$ and Contact resistance $R_C = \frac{\rho C}{A}$.

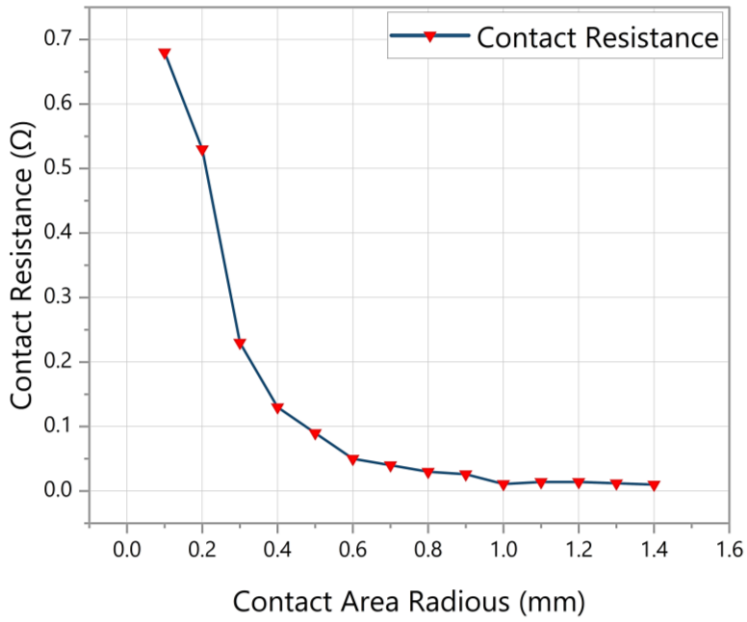

Figure 12. TEG circular copper contact geometry (mm) vs. contact resistance (Ω) analytical model

Here we observed that the electrical contacts of the thermoelectric generator in the copper area increased, the resistance decreased, the electrical conductivity increased, and the TEG efficiency increased. The contact area was varied from 0.1 mm in diameter to 1.5 mm in diameter. In the TEG module, the contact area was acceptable from 0.1 to 1.2 mm in diameter because the PN leg array space is 1.2 mm in diameter. In this geometry of contact design, the resistance decreased from 0.68Ω to 0.01Ω, corresponding to a varied geometry diameter from 0.1 mm to 0.5 mm. Subsequently, the values affect the slight changes in the electrical resistance of the contacts.

Case-3 Commercial TEG experiment block diagram

The purpose of this experiment is to investigate the thermoelectric generator through testing with a commercial module with different heat sources, required load resistances, and apparatuses to measure voltage, resistance, and current. A temperature gradient was created on the hot and cold sides of the thermoelectric generator module, and the voltage, current, and power produced by the module were recorded. The heat sink is eliminated for this purpose, and the ambient temperature is used as the cold-side temperature [23]. Notably, we did not consider the heat sink used and treated the ambient temperature as a reference for the cold side. The system registers temperature, voltage, resistance, and current using a data acquisition system.

Figure 13 shows a block diagram of a thermoelectric generator (TEG) experimental setup that provides a visual representation of the key components and their interactions used to study and evaluate the performance of the device. At the core of the setup is the thermoelectric module, which operates based on the Seebeck effect and converts temperature differences directly into electrical voltage. Enhanced heat management was achieved by heating one side of the module with a controlled source while cooling the other side to maintain a constant temperature difference in the module. Thermocouples or temperature sensors were placed on both sides to monitor the temperature difference (ΔT) in real time. The TEG parameters of the electrical output from the module were connected to a variable resistive load or a power measurement system, allowing for the evaluation of the voltage, current, and power output [5]. Data acquisition systems (DAQs) are often integrated to continuously record temperature and electrical parameters. This block diagram aids in understanding the functional flow of energy conversion and supports optimization studies of TEG efficiency under various operating conditions.

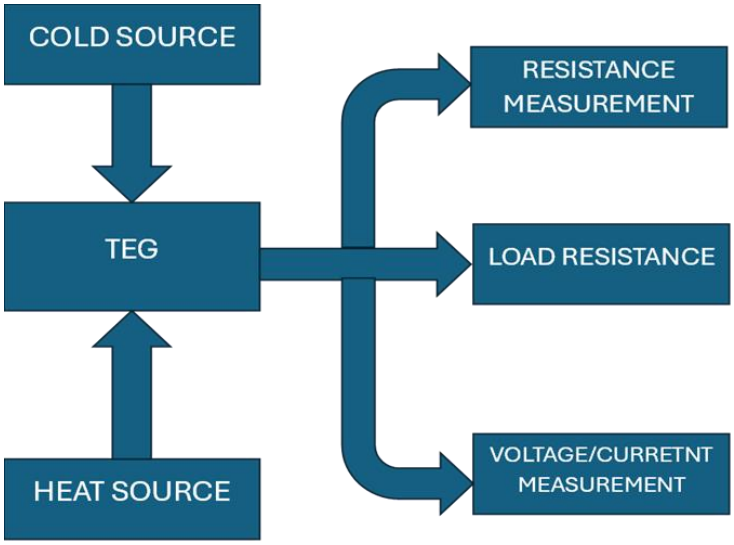

Figure 13. Block diagram of the experimental setup with the commercial TEG model system

4- Experimental Validation

Figure 14 shows that the electrical output and temperature difference were measured via thermocouples. Performance evaluations assess the improvement in TEG efficiency achieved through contact geometry optimization. The reduction in electrical contact resistance and its impact on the overall system performance are quantified. This methodology combines theoretical modeling, simulation, experimental [37] validation, and statistical analysis to systematically investigate and optimize the geometry of electrical contacts in thermoelectric generators, aiming to improve overall system efficiency. Design On the basis of these findings, new design guidelines for electrical contacts in TEG modules have been developed. These guidelines provide practical recommendations for future TEG manufacturing. The results suggest that the optimized contact geometry can be scaled for TEG systems. Potential applications in various industries were identified on the basis of improved efficiency [37]. The study shows that optimization of the geometry of electrical contact is essential if the efficiency of the TEG is to be increased, creating the possibility of moving forward with respect to clean energy technologies. Additionally, the Seebeck coefficient was taken to be constant, and the temperature differential between the ceramic and the legs was disregarded. Thermoelectric generator Efficiency:

$$\eta = \frac{P_{out}}{Q_{in}} \tag{15}$$

Geometry of different cases(dimensions) generating power P (Input power):

$$Q_{in} = \alpha I T_H - \frac{1}{2} I^2 R + K\Delta T \tag{16}$$

Equation 16 is the input temperature power Q_{in}, which depends on the thermoelectric generator parameters. Consider the electrical resistance R. Electrical Resistance (R) =0.26 Ω:

$$Generated\ power\ P = I^2 R \tag{17}$$

Here, the electrical power of the thermoelectric generator was calculated using Equation 17. Generated current $(I) = 5.1\ A$; Electrical conductivity $\sigma = 1.1 \times 10^5\ S\ m$; Thermal conductivity $k = 1.8\ WmK$; Temperature Gradient (ΔT), $\Delta T = T_H - T_C$; Seebeck coefficient, (α) = 190 μV/K.

Here, α is the Seebeck coefficient, R is the internal electrical resistance of the module, and K is the thermal conductance [21]. As the hot-side temperature increased above 298 K, the temperature gradient ΔT increased, leading to a higher thermoelectric voltage (from $V = \alpha \Delta T$) and subsequently a greater output power, assuming matched impedance. The experimental data consistently revealed an increase in efficiency with increasing Thot, confirming the theoretical prediction that efficiency improves with increasing ΔT. A temperature-controlled heater applied heat to the hot side, and the copper contacts facilitated electrical connections with minimal resistive losses. Thermocouples were embedded near both junctions to monitor the temperatures accurately. Using Equations 15 to 17, we calculated the thermoelectric output power and conversion efficiency, which are presented in Table 3.

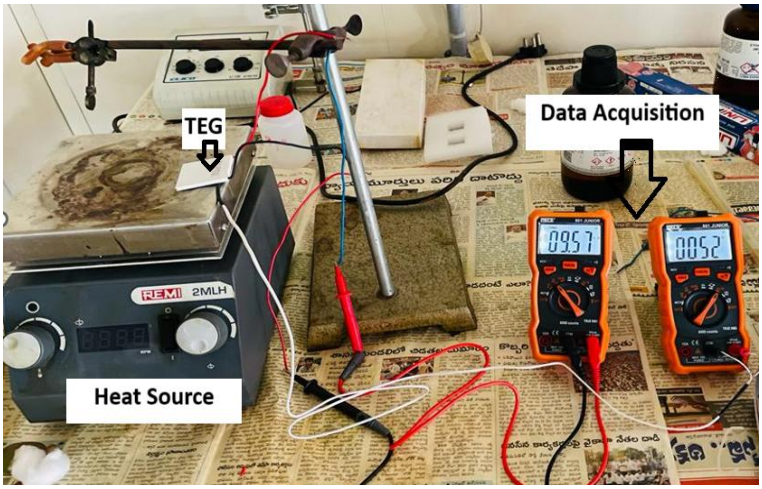

Figure 14. Experimental setup of the commercial TEG module, Heat source, Data acquisition

Table 3. Commercial thermoelectric generator, electrical contact, and resistance $R_c(\Omega)$ with different hot side temperatures (K) at room temperature (cold side) T_C = 298 K

Temperature T_H (K)	Contact Resistance (Ω)	TEG Efficiency (%)
298	3.5	0
300	3.1	1.6
302	2.8	2.3
304	2.4	3.1
306	1.8	4.2
308	1.63	4.8
310	1.54	5.3
312	1.41	5.9
314	1.39	6.3
316	1.36	6.7
318	1.30	6.9
320	1.23	7.2
322	1.12	7.6
323	1.10	7.9
324	0.98	8.3
326	0.86	8.7
328	0.73	9.1
400	**0.61**	**9.3**

Table 3 shows that the commercial thermoelectric resistance varies due to changes in the hot temperature. Here, from the experimental results, we observed that the contact resistance is the key factor affecting the TEG output power and conversion efficiency. Table 3 shows that commercial EG conversion efficiency improves with increasing temperature gradient through hot-side temperatures.

Figure 15 shows the commercial TEG experimental setup with various hot-side temperatures cold-side ambient temperatures and resistance variations. An important concern in the experimental analysis of TEG performance at low temperatures is evaluation of the impact of increasing the hot-side temperature on the electrical resistance of the device. and a variable hot source whose temperature was incrementally raised from a baseline near 298 K. As the temperature gradient ΔT decreased, the thermal energy supplied to the thermoelectric material enhanced the charge carrier mobility, thereby reducing the electrical resistance R of the TEG. The relationship between the resistance and temperature is described by the temperature-dependent resistivity.

$$R = \rho(T)\frac{L}{A} \quad (18)$$

where 'L' is the length and 'A' is the cross-sectional area of the conductor. For metals such as copper used in contact interfaces, the resistivity decreases with increasing temperature up to a certain point, which is often approximated by a linear relationship.

$$\rho(T) = \rho_0[1+\alpha(T-T_0)] \quad (19)$$

where ρ_0 is the resistivity at a reference temperature, usually 298 K, and α\alphaα is the temperature coefficient of the resistivity. By gradually increasing T_HThis setup exploits the favorable thermal activation of the carriers, effectively reducing the resistance and improving the power output.

$$P = \frac{V^2}{R} \quad (20)$$

Here, a decrease in resistance R leads to a higher power output for a given voltage V. This behavior is particularly important for optimizing the TEG efficiency.

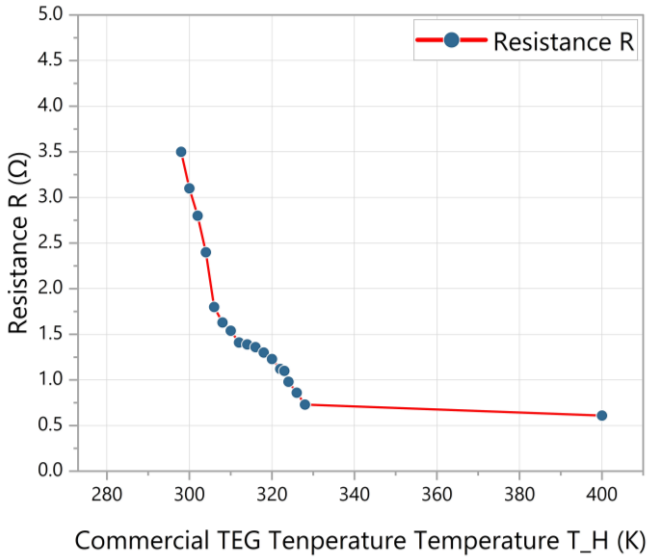

Figure 15. Experimental setup of the commercial TEG model: electrical resistance vs. TEG efficiency (%) variations with different hot temperatures at a cold temperature of T_C = 298 K

5- Results and Discussion

Figure 16 shows a graph commercial the TEG temperature versus TEG conversion efficiency. In this experimental study, the TEG was characterized. We observed this phenomenon under low-temperature conditions focusing on how variations in the hot-side input temperature affect the overall efficiency. The system was configured with a fixed cold-side temperature maintained at approximately 298 K (room temperature), while the hot-side temperature was incrementally increased to assess its impact on the power output and thermoelectric conversion efficiency.

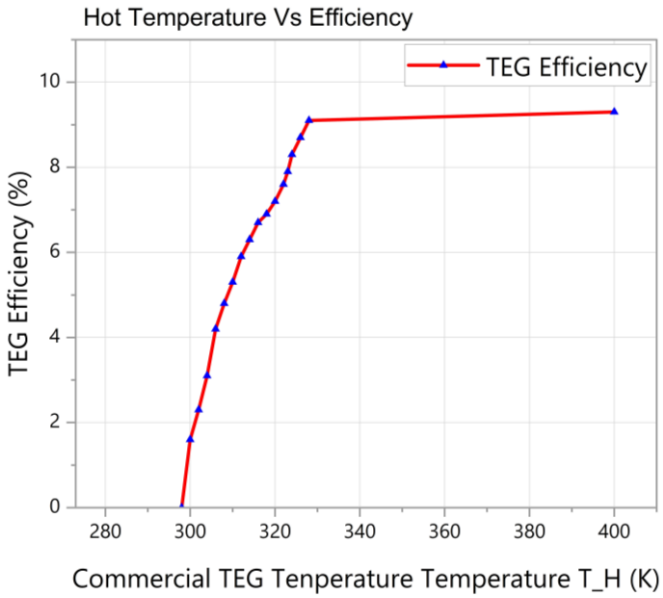

Figure 16. Experimental setup of the commercial TEG model: Hot temperature(K) vs. TEG efficiency (%) variations at a cold temperature of T_C = 298 K

5-1- Comparison with Commercial TEGs

Compared to the numerical model, the analytical model results in greater discrepancies between the temperature and resistance, output power, and efficiency values (Figures 11 and 12), which yields results that are more closely aligned with the manufacturer's datasheet data. This discrepancy arises from the implementation of the calculation's analytical equations, which are not present in the numerical analytical model, as previously discussed in the methodology, including the calculation of the contact resistance. The improved thermoelectric generator (TEG) efficiency resulting from the optimization of the electrical contact geometry demonstrates significant performance advancements, reducing the contact resistance [8]. The contact resistance of the base TEG module reduced power. Here, the optimized contact geometry leads to substantially decreased electrical contact resistance.

From Table 4, a comparative analysis of different TEG contact designs indicated that the surface shape changed and improved the mechanical conformity, thus lowering the resistance without the loss of the generated TEG power. Comparison of flat contact and circular contact with a commercial TEG. The results show an 18.6% increase in system efficiency with the proposed design modifications of TEG copper contacts in the shape of a circular area $7.85\times10^{-7}mm^2$.

Table 4. Comparison of the measured contact resistance (Ω) of different shapes at T=323 k

Method	Contact Geometry	Contact Resistance (Ω)	TEG Efficiency (%)
Flat (mm)	0.1	0.08	12.2
	0.5	0.18	9.4
	1.0	0.47	8.3
Proposed Circular (mm^2)	0.1	1.68	12.6
	0.5	0.097	17.8
	1.0	0.011	18.6
Existing Method: cascaded TEG [4]	2 (mm^2)	6×10^{-10}	8.46
	3 (mm^2)	3×10^{-10}	9.26
	4 (mm^2)	8×10^{-10}	7.66
Existing Method: Elements Quantity [5]	10 mm	16	8
Existing Method [5]	-	-	8.8
Experimental Commercial TEG at T_H =323K, T_C=293K	-	3.10	7.9

As shown in Table 4 compared with traditional flat-type contact geometries used in existing systems and commercial TEG setups, the thermoelectric generator (TEG) demonstrated an 18.6% improvement in efficiency when circular copper electrical contacts were employed. This enhancement is attributed primarily to the reduced electrical resistance and increased electrical conductivity associated with the larger contact area provided by the circular geometry. The improved contact configuration facilitates more efficient charge carrier flow, leading to better overall energy conversion performance under identical thermal conditions.

Compared with conventional designs, a measurable increase in voltage and current generation was observed. Improved Conversion Efficiency. The optimized contact geometry contributed to a higher thermoelectric conversion efficiency. The efficiency improvement was quantified and compared with baseline measurements. With respect to thermal management, the new contact design resulted in better heat distribution and reduced thermal resistance. This led to more effective temperature gradient maintenance across the thermoelectric elements. In conjunction with the simulations, the experimental results closely matched the predictions from COMSOL Multiphysics simulations. This validation strengthens the reliability of the theoretical model and the simulation approach. Statistical analysis confirmed the significance of the efficiency improvements. These results are consistent across multiple trials, indicating reproducibility.

6- Conclusion

This study addresses the primary disadvantage of thermoelectric generators: their low conversion efficiency, which is attributed to poor electrical conductance. The contact resistances of thermoelectric generators significantly affect the electrical conductance of the generated output power and, consequently, the conversion efficiency. To investigate the impact of electrical contact resistance, thermoelectric generators with various contact geometries and shapes (flat and circular) were designed to enhance performance. Experiments were conducted using commercial TEGs, examining the existing contacts and their electrical contact resistances. The designed contact geometries and shapes were then compared by assessing electrical contact resistance and evaluating output power and conversion efficiency.

The findings indicate that circular copper contacts in thermoelectric generators result in higher output performance. As the electrical contact resistance decreases, the output voltage, output power, and conversion efficiency of the TEG increase. Previous studies have also demonstrated the advantages of circular designs in thermoelectric generators. One study reported an 18.6% increase in net power when circular copper contacts with an area of 7.85×10^{-7} mm² significantly reduced contact resistance. The use of circular-shaped copper contacts for multiple electrical connections further indicates that circular geometries can enhance overall performance.

7- Nomenclatures

A_C	Cross-sectional area of contacts (mm^2)	L	Length of the contacts / thickness of the contacts (mm)
D	Diameter (mm)	I	Current (A)
R	Resistance (Ω)	R_C	Contact resistance (Ω)
P	Output power (W)	Q	Heat absorption power (W)
R_{TEG}	Internal resistance (Ω)	R_L	Load resistance (Ω)
T	Temperature (K)	T_H	Hot temperature (K)
T_C	Cold temperature (K)	ZT	Figure of merit of the thermoelectric generator
V	Voltage (V)	V_{oc}	Open circuit voltage (V)
I_{oc}	Open circuit current (A)	Eff	Effectiveness
TEG	Thermoelectric generator	DAQs	Data Acquisition Systems
α	Seebeck coefficient (V/K)	ρ	Resistivity
σ	Conductivity (S/m)	Δ	Difference
η	Efficiency (%)	∴	Therefore
H	Hot	C	Cold
L	Load	n	n-leg
p	p-leg	1	Case-1
2	Case-2	3	Case-3

8- Declarations

8-1- Author Contributions

Conceptualization, N.J.B. and R.K.B.; methodology, N.J.B.; software, N.J.B.; validation, N.J.B. and R.K.B.; formal analysis, N.J.B.; investigation, N.J.B.; resources, N.J.B.; data curation, N.J.B.; writing—original draft preparation, N.J.B.; writing—review and editing, N.J.B.; visualization, N.J.B.; supervision, R.K.B.; project administration, R.K.B.; funding acquisition, R.K.B. All authors have read and agreed to the published version of the manuscript.

8-2- Data Availability Statement

The data presented in this study are available on request from the corresponding author.

8-3- Funding

The authors received no financial support for the research, authorship, and/or publication of this article.

8-4- Acknowledgments

The authors of this research article are thankful to GITAM, deemed to be University, Visakhapatnam, Andhra Pradesh, India, for extending their support.

8-5- Institutional Review Board Statement

Not applicable.

8-6- Informed Consent Statement

Not applicable.

8-7- Conflicts of Interest

The authors declare that there is no conflict of interest regarding the publication of this manuscript. In addition, the ethical issues, including plagiarism, informed consent, misconduct, data fabrication and/or falsification, double publication and/or submission, and redundancies have been completely observed by the authors.

9- References

[1] Li, Y., Shi, Y., Wang, X., Luo, D., & Yan, Y. (2023). Thermal and electrical contact resistances of thermoelectric generator: Experimental study and artificial neural network modelling. Applied Thermal Engineering, 225, 120154. doi:10.1016/j.applthermaleng.2023.120154.

[2] Tang, H., Bai, H., Yang, X., Cao, Y., Tang, K., Zhang, Z., Chen, S., Yang, D., Su, X., Yan, Y., & Tang, X. (2022). Thermal stability and interfacial structure evolution of Bi2Te3-based micro thermoelectric devices. Journal of Alloys and Compounds, 896, 163090. doi:10.1016/j.jallcom.2021.163090.

[3] Dalkiranis, G. G., Bocchi, J. H. C., Oliveira, O. N., & Faria, G. C. (2023). Geometry Optimization for Miniaturized Thermoelectric Generators. ACS Omega, 8(10), 9364–9370. doi:10.1021/acsomega.2c07916.

[4] Luo, Y., & Kim, C. N. (2019). Effects of the cross-sectional area ratios and contact resistance on the performance of a cascaded thermoelectric generator. International Journal of Energy Research, 43(6), 2172–2187. doi:10.1002/er.4426.

[5] Chen, B., Wu, Y. D., Ma, W. G., & Guo, Z. Y. (2025). Experimental verification of one-dimensional models of thermoelectric generators. Physical Review E, 111(4), 45506. doi:10.1103/PhysRevE.111.045506.

[6] Coelho, R., De Abreu, Y., Carvalho, F., Branco Lopes, E., & Gonçalves, A. P. (2022). An Electrical Contacts Study for Tetrahedrite-Based Thermoelectric Generators. Materials, 15(19), 6698. doi:10.3390/ma15196698.

[7] Liao, J., Xie, H., Wang, J., Sun, L., Long, X., Li, C., Gao, T., Xia, E., & Liu, Z. (2025). Efficient performance analysis and optimization of thermoelectric generators for low-grade heat sources: A simplified equivalent numerical modeling approach. Energy, 320, 135474. doi:10.1016/j.energy.2025.135474.

[8] Lekbir, A., Mekhilef, S., Tey, K. S., & Albaker, A. (2025). Performance and environmental impact analysis of thermoelectric generators through material selection and geometry optimization. Energy Materials, 5(8), 46. doi:10.20517/energymater.2025.46.

[9] Wang, H., Wang, W., Li, G., Waktole, D. A., Zuo, Z., Jia, B., Feng, H., Wang, M., & shao, S. (2025). High-performance flexible thermoelectric generator with hydrogel-copper foam cooling for self-powered wearable electronics. Case Studies in Thermal Engineering, 74, 106835. doi:10.1016/j.csite.2025.106835.

[10] Kramer, L. R., Maran, A. L. O., De Souza, S. S., & Ando, O. H. (2019). Analytical and numerical study for the determination of a thermoelectric generator's internal resistance. Energies, 12(16), 3053. doi:10.3390/en12163053.

[11] Doraghi, Q., & Jouhara, H. (2024). Thermoelectric generator efficiency: An experimental and computational approach to analysing thermoelectric generator performance. Thermal Science and Engineering Progress, 55, 102884. doi:10.1016/j.tsep.2024.102884.

[12] Bhatt, R., Bohra, A. K., Bhattacharya, S., Basu, R., Ahmad, S., Singh, A., Muthe, K. P., & Gadkari, S. C. (2017). Optimisation of electrical contact resistance in Bi0.5Sb1.5Te3 for development of thermoelectric generators. AIP Conference Proceedings, 1832, 60021. doi:10.1063/1.4980426.

[13] Tripathi, A., Dhar, A., & Pandey, S. K. (2022). Optimization of hybridization strategy for improving the efficiency of thermoelectric generator to recover automobile exhaust waste heat. Engineering Research Express, 4(1), 015017. doi:10.1088/2631-8695/ac5126.

[14] Pennelli, G., Dimaggio, E., & Macucci, M. (2022). Electrical and thermal optimization of energy-conversion systems based on thermoelectric generators. Energy, 240, 122494. doi:10.2139/ssrn.3884852.

[15] Yuan, C., Sadashivaiah, G., Bechtold, T., & Rudnyi, E. B. (2019). Efficient design optimization of a thermoelectric generator by a combination of model order reduction and thermal submodeling techniques. Proceedings - European Council for Modelling and Simulation, ECMS, 33(1), 290–295. doi:10.7148/2019-0290.

[16] Yuan, C., Kreß, S., Sadashivaiah, G., Rudnyi, E. B., Hohlfeld, D., & Bechtold, T. (2020). Towards efficient design optimization of a miniaturized thermoelectric generator for electrically active implants via model order reduction and submodeling technique. International journal for numerical methods in biomedical engineering, 36(4), e3311. doi:10.1002/cnm.3311.

[17] Bekhouche, D., Bouchoucha, A., & Zaidi, H. (2024). Optimization of Friction and Electrical Resistance Performance in Graphite-Copper Electrical Contacts Using Taguchi-based Grey Relational Analysis. FME Transactions, 52(4), 628–638. doi:10.5937/fme2404628B.

[18] Tian, L., Chen, L., Ge, Y., & Shi, S. (2022). Maximum Efficient Power Performance Analysis and Multi-Objective Optimization of Two-Stage Thermoelectric Generators. Entropy, 24(10), 1443. doi:10.3390/e24101443.

[19] Jaafar, A. H., & Al-Ethari, H. (2020). Optimization of manufacturing copper-graphite composite for electrical contact applications using grey relational analysis. Materiaux et Techniques, 108(1), 101. doi:10.1051/mattech/2020013.

[20] Solovev, B. A., Gamisonia, G. K., Dimukasheva, G. Y., & Kolomeets, D. A. (2024). Conversion of Thermal Energy into Electricity: Potential and Efficiency of Thermoelectric Generators Based on Peltier Elements. Electrical and Data Processing Facilities and Systems, 20(1), 55–64. doi:10.17122/1999-5458-2024-20-1-55-64.

[21] Egypt, P., Sakdanuphab, R., Sakulkalavek, A., Klongratog, B., & Somdock, N. (2024). Optimizing Waste Heat Conversion: Integrating Phase-Change Material Heatsinks and Wind Speed Dynamics to Enhance Flexible Thermoelectric Generator Efficiency. Materials, 17(2), 420. doi:10.3390/ma17020420.

[22] Voloshchuk, I. A., & Terekhov, D. Y. (2021). Investigation of the Electrical Contact to the Thermoelectric Legs Fabricated by Screen-printing Method. Proceedings of the 2021 IEEE Conference of Russian Young Researchers in Electrical and Electronic Engineering, ElConRus 2021, 2501–2505. doi:10.1109/ElConRus51938.2021.9396295.

[23] Doraghi, Q., Khordehgah, N., Żabnieńska-Góra, A., Ahmad, L., Norman, L., Ahmad, D., & Jouhara, H. (2021). Investigation and computational modelling of variable teg leg geometries. ChemEngineering, 5(3), 45. doi:10.3390/chemengineering5030045.

[24] Alghamdi, H., Maduabuchi, C., Okoli, K., Albaker, A., Alobaid, M., Alghassab, M., Makki, E., & Alkhedher, M. (2024). Bayesian neural networks for solar power forecasts in advanced thermoelectric systems. Case Studies in Thermal Engineering, 61, 104940. doi:10.1016/j.csite.2024.104940.

[25] Park, N. W., Park, T. H., Ahn, J. Y., Kang, S. H., Lee, W. Y., Yoon, Y. G., Yoon, S. G., & Lee, S. K. (2016). Thermoelectric characterization and fabrication of nanostructured p-type Bi0.5Sb1.5Te3 and n-type Bi2Te3 thin film thermoelectric energy generator with an in-plane planar structure. AIP Advances, 6(6), 65123. doi:10.1063/1.4955000.

[26] Liu, Q. Y., Shi, X. L., Cao, T. Y., Chen, W. Y., Li, L., & Chen, Z. G. (2025). Advances and challenges in inorganic bulk-based flexible thermoelectric devices. Progress in Materials Science, 150, 101420. doi:10.1016/j.pmatsci.2024.101420.

[27] Chen, J., Li, K., Liu, C., Li, M., Lv, Y., Jia, L., & Jiang, S. (2017). Enhanced efficiency of thermoelectric generator by optimizing mechanical and electrical structures. Energies, 10(9), 1329. doi:10.3390/en10091329.

[28] Selvan, K. V., Rehman, T., Saleh, T., & Ali, M. S. M. (2019). Copper-Cobalt Thermoelectric Generators: Power Improvement Through Optimized Thickness and Sandwiched Planar Structure. IEEE Transactions on Electron Devices, 66(8), 3459–3465. doi:10.1109/TED.2019.2920898.

[29] Snyder, G. J., & Toberer, E. S. (2008). Complex thermoelectric materials. Nature Materials, 7(2), 105–114. doi:10.1038/nmat2090.

[30] Li, Y., Bai, S., Wen, Y., Zhao, Z., Wang, L., Liu, S., Zheng, J., Wang, S., Liu, S., Gao, D., Liu, D., Zhu, Y., Cao, Q., Gao, X., Xie, H., & Zhao, L. D. (2024). Realizing high-efficiency thermoelectric module by suppressing donor-like effect and improving preferred orientation in n-type Bi2(Te, Se)3. Science Bulletin, 69(11), 1728–1737. doi:10.1016/j.scib.2024.04.034.

[31] Yusuf, A., Bayhan, N., Ibrahim, A. A., Tiryaki, H., & Ballikaya, S. (2021). Geometric optimization of thermoelectric generator using genetic algorithm considering contact resistance and Thomson effect. International Journal of Energy Research, 45(6), 9382–9395. doi:10.1002/er.6467.

[32] Zhu, T., Liu, Y., Fu, C., Heremans, J. P., Snyder, J. G., & Zhao, X. (2017). Compromise and Synergy in High-Efficiency Thermoelectric Materials. Advanced Materials, 29(14), 1605884. doi:10.1002/adma.201605884.

[33] Murmu, P. P., & Kennedy, J. (2023). Energy harvesting from ambient heat sources using thermoelectric generator – A modelling study. Materials Today: Proceedings, 528. doi:10.1016/j.matpr.2023.03.528.

[34] Arora, R., Kaushik, S. C., & Arora, R. (2016). Thermodynamic modeling and multi-objective optimization of two stage thermoelectric generator in electrically series and parallel configuration. Applied Thermal Engineering, 103, 1312–1323. doi:10.1016/j.applthermaleng.2016.05.009.

[35] He, J., & Tritt, T. M. (2017). Advances in thermoelectric materials research: Looking back and moving forward. Science, 357(6358), 9997. doi:10.1126/science.aak9997.

[36] Wu, C. I., Du, K. W., & Tu, Y. H. (2024). Enhanced Energy Harvesting from Thermoelectric Modules: Strategic Manipulation of Element Quantity and Geometry for Optimized Power Output. Energies, 17(21), 5453. doi:10.3390/en17215453.

[37] Shittu, S., Li, G., Zhao, X., Ma, X., Akhlaghi, Y. G., & Fan, Y. (2020). Comprehensive study and optimization of concentrated photovoltaic-thermoelectric considering all contact resistances. Energy Conversion and Management, 205, 112422. doi:10.1016/j.enconman.2019.112422.